Consiglio Nazionale delle Ricerche
Istituto di Matematica Applicata
e Tecnologie Informatiche
“Enrico Magenes”

REPORT SERIES

Chiara Romanengo, Silvia Biasotti, Bianca Falcidieno

Recognising characteristic elements through the analysis of curves on 3D models

19-01

IMATI REPORT Series

Nr. 19-01
27 May, 2019

IMATI Report Series Nr. 19-01
May 27, 2019

Recognising characteristic elements through the analysis of curves on 3D models

Chiara Romanengo, Silvia Biasotti, Bianca Falcidieno

Chiara Romanengo
Dipartimento di Matematica
Università degli Studi di Genova
Via Dodecaneso 35 - 16146 Genova, Italy
E-mail: chiara.romanengo@gmail.com

Silvia Biasotti
Istituto di Matematica Applicata e Tecnologie Informatiche "E. Magenes"
Consiglio Nazionale delle Ricerche
Via de Marini, 6 (Torre di Francia) - 16149 Genova, Italy
E-mail: silvia@ge.imati.cnr.it

Bianca Falcidieno
Istituto di Matematica Applicata e Tecnologie Informatiche "E. Magenes"
Consiglio Nazionale delle Ricerche
Via de Marini, 6 (Torre di Francia) - 16149 Genova, Italy
E-mail: bianca.falcidieno@ge.imati.cnr.it

Abstract.

We propose a new method for recognising characteristic curves on 3D shapes, identified by a set of characteristic points. We approximate these curves with known curves, e.g., spirals, their patterns or aggregations, to provide a localisation and quantitative measurement of style features like decorations, visual motifs or anatomical features on the digital models of 3D objects. To solve this problem, we adopt a generalisation of the Hough Transform (HT) which is able to deal with curves represented either in implicit and parametric form and extends the set of curves so far adopted for curve recognition with HT. In addition, we introduce new rules of composition and aggregation of characteristic curves into patterns or decorations, not limiting the recognition to a single curve at a time.
Besides planar curves, our method yields the recognition of spatial curves (see Figure 1): to the best of our knowledge, this is the first attempt to apply the HT to the recognition of spatial curves without any projection onto a fitting plane.

Keywords: *Feature curves, Hough transform, characteristic elements*

Recognising characteristic elements through the analysis of curves on 3D models

Chiara Romanengo, Silvia Biasotti, Bianca Falcidieno

Abstract

We propose a new method for recognising characteristic curves on 3D shapes, identified by a set of characteristic points. We approximate these curves with known curves, e.g., spirals, their patterns or aggregations, to provide a localisation and quantitative measurement of style features like decorations, visual motifs or anatomical features on the digital models of 3D objects. To solve this problem, we adopt a generalisation of the Hough Transform (HT) which is able to deal with curves represented either in implicit and parametric form and extends the set of curves so far adopted for curve recognition with HT. In addition, we introduce new rules of composition and aggregation of characteristic curves into patterns or decorations, not limiting the recognition to a single curve at a time. Besides planar curves, our method yields the recognition of spatial curves (see Figure 1): to the best of our knowledge, this is the first attempt to apply the HT to the recognition of spatial curves without any projection onto a fitting plane.

1 Introduction

Style is mainly a property of man-made objects (artefacts or handcrafts), it defines a characteristic way of doing things that is peculiar to a specific time, place or designer. An object's style is strongly related to its visibility, since objects which

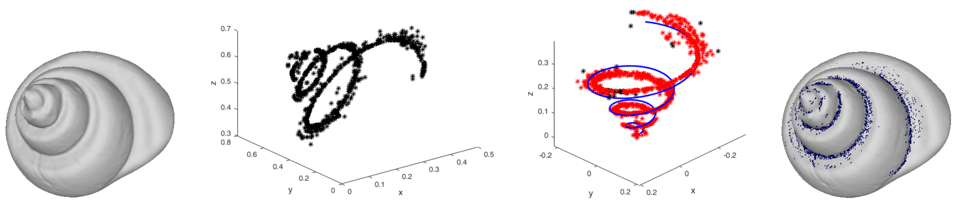

(a) (b) (c) (d)

Figure 1: A digital model of a shell (a), the set of characteristics points in (b) is recognised with the Hough transform as a helix curve in (c). In (d) the points that best fit with the curve recognised are highlighted on the model.

are not publicly visible usually show little stylistic variability due to their inability to transmit public messages [Ran81]. In the *visual* arts, styles are regarded as distinctive and recognisable forms which permit the grouping of works containing these forms into analogous categories [Wikipedia]. Human notions of style are typically conceived at a high level and stated in vague terms [HLK*17]. Thus, the characterisation of individual style is inherently abstract, ambiguous and subjective. Difficult to be formally defined, it is often viewed as a residual category in the description of 3d shapes. However, style is an important aspect to consider when checking similarities between objects, prompting the inevitable question of how styles can be concretely extracted or described. The human perception of style similarity transcends function, structure and also overall shape. Objects that are stylistically similar can have a strong variance in these elements. For example, a table and a chair, a vase and a dish, or a helmet and a cuirass may share a common style.

In the digital era, where the differences of style cannot be always judged by a human expert, it is necessary to translate general and vague style definitions into something measurable in order to evaluate compatibility between objects. Quantifying human perception of style of 3D shapes is crucial for many applications. There has been a recent interest in research in style-based similarity metrics of 3D content for interior design [LKWS16, HLK*17], architecture [BLL15], archaeology [RES16], arts and aesthetics [DKVL16]. Also in some natural forms like shells, flowers and leaves sometimes we use it to identify peculiar shapes [HT11].

Style can be referred to an object's global shape (e.g. round, sharp. smooth, crisp), or to its style defining elements, called style features or patterns ([TBF18, MTB18, MTB19]), characteristic lines [APM15], decorations [RES16] or visual motifs [KKF91]. In particular, characteristic curves or lines play an important role in the perception of a shape style [HT11].

Contribution In this paper we focus on recognising style curves on 3D shapes, represented as curve segments identified by a set of vertices and approximated with known curves, like spirals, their patterns or aggregations, which characterise style features like decorations, visual motifs or anatomical features on the digital models of 3D objects.

The focus here is on the extraction of characteristic curves from a set of potentially significant points using a generalisation of the Hough Transform (HT) [BR12], already introduced in a recent paper [TBF18]. This technique takes advantage of a rich family of primitive curves that are flexible to meet the user needs. The method recognises various features, possibly compound, and selects the most suitable profile among families of curves. Deriving from the HT, the method inherits the robustness to noise and the capability of dealing with data incompleteness as for the degraded and broken 3D artefacts.

We introduce a generalised and extended approach of the previous method [TBF18], by proposing a technique able to:

- deal with curves represented either in implicit and parametric form;
- add new curves in the set of curves successfully treated with the Hough transform. A vast catalogue of functions is already available in [TBF18], and we show how to extend it provided that the new curve is expressed in parametric or algebraic form;
- define new rules of composition and aggregation of characteristic curves into patterns or decorations;
- evaluate the goodness of the curve approximation (GoF);
- deal with spatial curves, like the helix of Figure 2. To the best of our knowledge this is the first attempt to apply the HT to the recognition of spatial curves without any projection onto a fitting plane.

Organisation The remainder of the paper is organised as follows. In Section 2, we briefly review previous research in style characterisation and curve recognition. Section 3 introduces the Hough transform for curves. Section 4 describes the method in detail and how the HT concept may tackle spatial curves. Section 5 shows the results of the method applied to real 3D scans, recently proposed in an international contest (SHREC'19 [MGM*19]).

2 State of the art

2.1 Style characterisation

A mainstream strategy to address the characterisation of style elements is to adopt learning strategies [LKS15,LKWS16]; for instance, defining the style-defining elements as recurring elements, co-located over a class of geometric shapes [HLK*17]. Being based on a number of positive examples (for instance, obtained with crowd sourcing strategies), these methods classify one design style at a time. Still limited to images, the work in [DSG*12] combines geotagged images and learning approaches to automatically detect the elements of architectural style of a component (windows, balconies, street signs, etc.). Learning algorithms can be applied to study how the perceptual grouping of features is based on the encoding of elements' shape, context, symmetries, and structural arrangements. This approach has been recently proposed in [LZH*17] for image patterns, where authors used different convolutional neural networks trained to recover structure, context and symmetry information of a pattern. Learning approaches are definitely interesting and powerful, however, they seem to be scarcely applicable to Cultural Heritage domain, primarily for the lack of training data and for the incompleteness of artefacts.

Related to architecture, the approach proposed in [BLL15] adopts a bottom-up strategy to characterise the features of a collection of columns starting with the identification of straight lines with the standard HT. In addition, many works developed for shape retrieval or shape similarity have some analogy with these approaches, but it is important to underline once more that object similarities do not necessarily correspond to style similarities. However, some previous papers describe techniques potentially useful to identify style-discriminating or style-defining elements in shape models; for instance, we can cite the works developed in [RES16, Tal14] in the contest of Cultural Heritage or methods for shape correspondence and symmetry analysis [KZHCO11, MPWC12].

2.2 Recognition of curves

Characteristic curves are a popular tool for visual shape illustration [KST08] and perception studies support these curves as an effective choice for representing the salient parts of a 3D model [CGL*08, HT11].

In general, given a set of (feature) points, the curve fitting problem is largely addressed in the literature, [Far93, Shi95, PT97, DIOHS08]. Among the others, [APM15] recently grouped the salient points into a curve skeleton that is fitted with a quadratic spline approximation. Being based on a local curve interpolation, such a class of methods is not able to recognise entire curves, to complete missing parts, and to assess if a feature is repeated at different scales.

Besides interpolating approaches such as splines, it is possible to fit the feature curve set with some specific family of curves. For instance the *natural 3D spiral* [HT11] and the *3D Euler spiral* [HT12] have been proposed as a natural way to describe line drawings and silhouettes showing their suitability for shape completion and repair. However, using one family of curves at a time implies the need of defining specific solutions and algorithms for settings the curve parameters during the reconstruction phase.

Recently, characteristic curves identification has been addressed with co-occurrence analysis approaches [SJW*11, LWWS15]. In this case, the curve learning process is applied to a set of characteristic points. The learning phase is interactive and requires 2-3 training examples for every type of curve to be identified and sketched; in case of multiple curves it is necessary also to specify salient nodes for each curve. Characteristic lines are poly-lines (i.e. connected sequences of segments) and do not have any global equation. These methods are adopted mainly for recognising parts of buildings (such as windows, doors, etc.) and features in architectural models that are similar to strokes. Main limitations of these methods are the partial tolerance to scale variance, the need of a number of training curves for each class of curves, the non robustness to missing data and the fact that compound features can be addressed only one curve at a time [SJW*11].

2.3 Hough transform

The Hough Transform (HT) is a standard pattern recognition technique originally used to detect straight lines in images, [Hou62, DH72]. Since its original conception, the HT has been extensively used and many generalisations have been proposed for identifying instances of arbitrary shapes over images [Bal81], or, more commonly, circles or ellipses. For a detailed analysis of the HT we refer to these surveys [MC15, KTT99]). The Standard Hough Transform (SHT), as currently known, was defined in [DH72]. It concerns the detection of any parametric, analytic, planar curve. In spite of its robustness, its use has been limited by the need of a parametric expression, the dependence of the computation time and the memory requirements on the number of curve parameters, and even the need of a finer parameters quantisation for a higher accuracy of results. The Generalised Hough Transform (GHT) [Bal81] overcomes the need of a parametric analytic expression and works on a generic, planar shape. Thus, the GHT is more general than SHT, as it is able to detect a larger class of rigid objects, still retaining the robustness of SHT. Nevertheless, the GHT adopts a brute force approach that enumerates all the possible orientations and scales of the input shape, thus the number of parameters in its process is considerably high and prevent its adoption in the 3D space. Further, the GHT cannot adequately handle similar shapes, as in the case of different instances of the same shape, which are comparable but not identical, e.g. petals and leaves.

Thanks to algebraic geometry concepts, theoretical foundations have been laid to extend the HT technique to the detection of algebraic objects of co-dimension greater than one (for instance algebraic space curves) taking advantage of various families of algebraic planar curves (see [BR12] and [BMP13]). Being so general, such a method allows dealing with different shapes, possibly compound [TBF18], and to get the most suitable approximating profile among a large vocabulary of curves [Shi95].

In 3D, other variants of HT have been introduced and used, but as far as we know none of them exploits the huge variety of curves. For instance, in [OLA14] the HT has been employed to identify recurring straight line elements on the walls of buildings. In that application, the HT is applied only to planar point sets and line elements are clustered according to their angle with respect to a main wall direction; in this sense, the Hough aggregator is used to select the feature line directions (horizontal, vertical, slanting) one at a time. More recently, [TBF18] has proposed an implementation of the theory described in [BR12] and [BMP13] for curves in the space that can be modelled as the intersection of a surface and a plane. Taking advantage of the assumption that characteristic curves can be locally projected onto a fitting plane, the HT is evaluated for a planar curve and then re-projected on the object surface. To evaluate the accumulation matrix from an implicit curve representation, the approximation bounds in [TB14] were adopted. The method showed its effectiveness for the recognition of features and decorations over a number of artefacts and archaeological fragments.

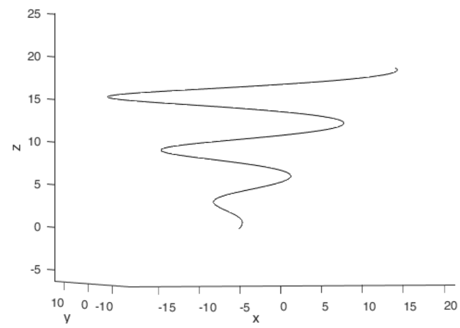

Figure 2: A conical helix

3 Hough transform for curves

This Section summarises the basic concepts behind the HT, its formulation for implicit and parametric curves and, finally, it focuses on a set of non-trivial curves that we adopt in our experiments.

3.1 Preliminary concepts

In general, a curve is defined through a continuous function $\gamma : I \to X$ from an interval I of the real numbers into a topological space X. In other words, a curve is a topological space which is locally *homeomorphic* to a line [Lip69]. In case X is of three dimensions, such as the Euclidean space, the curve is called *spatial*, while if X is a plane, the curve is called *planar*. Spatial curves that do not lie on a plane are called *skew* curves.

To be analytically represented, spatial curves must be expressed as the intersection of at least two surfaces. Their recognition is a problem of curve fitting for a given set of points or approximating a curve for these data points. Differently from planar curves that need only one equation and can count on large atlases of basic curves, e.g., [Shi95], spatial curves are much less codified. An example of spatial curve is the conical helix in Figure 2. In parametric form, a conical helix is represented by the equation: $\gamma(t) = (t\cos(t), t\sin(t), t)$.

In the plane, it is well-known that the HT is based on the *point-line duality* as follows: points on a straight line, defined by an equation, correspond to lines in the parameter space that intersect in a single point. This point uniquely identifies the coefficients in the equation of the original straight line. In general, the duality concept extends to curves in the space represented as the zero locus of a finite collection of real analytic functions [TBS18]. Given a family $\mathcal{F}$ of curves, a general point P in the space corresponds to a locus, $\Gamma_P(\mathcal{F})$, in the parameter space. The families $\mathcal{F}$ such that, as P varies on a given curve $\mathcal{C}$ from $\mathcal{F}$, satisfy the regularity condition that the hypersuperfaces $\Gamma_P(\mathcal{F})$ meet in one and only one point (which in turn defines the curve $\mathcal{C}$), are called *Hough regular*.
In case of algebraic curves, it is possible to explicitly verify if the curve is HT-

regular and therefore, the HT accumulation point is unique [BR12]. In case the HT regularity is not guaranteed, the accumulation point might be non unique and the user has to select among more potential parameter solutions.

For instance, considering the family $\mathcal{F} = \{\mathcal{C}_{a,b,c}\}$ of the conical helix represented by the implicit equation

$$\mathcal{C}_{a,b,c} : \begin{cases} \frac{x^2}{a^2} + \frac{y^2}{b^2} - \frac{z^2}{c^2} = 0 \\ x = a\frac{z}{c}\cos(\frac{z}{c}) \end{cases},$$

the Hough transform of a point $P = (x_P, y_P, z_P)$ with respect to the family $\mathcal{F}$ is the locus

$$\Gamma_P(\mathcal{F}) : \begin{cases} C^2B^2x_P^2 + C^2A^2y_P^2 - A^2B^2z_P^2 = 0 \\ x_P = A\frac{z_P}{C}\cos\left(\frac{z_P}{C}\right) \end{cases}.$$

If a family of curves is represented in parametric form, the HT can be derived directly from the parametric curve equations when the system admits an analytical solution. For instance, in the case of helices, a parametric form is provided by the following equation:

$$\mathcal{C}_{a,b,c} : \begin{cases} x = at^n\cos t \\ y = bt^n\sin t \qquad t \in \mathbb{R}, \\ z = ct^m \end{cases} \tag{1}$$

where n and m are rational numbers and a, b and c are parameters of the family of curves. Then, the parametric form of the HT of a point $P = (x_P, y_P, z_P)$ can be derived by solving the linear system with respect to the parameters a, b and c and it assumes the following expression:

$$\Gamma_P(\mathcal{F}) : \begin{cases} A(t) = \dfrac{\begin{vmatrix} x_P & 0 & 0 \\ y_P & t^n\sin t & 0 \\ z_P & 0 & t^m \end{vmatrix}}{D(t)} = \frac{x_P t^{n+m}\sin t}{D(t)} = \frac{x_P}{t^n\cos t} \\ B(t) = \dfrac{\begin{vmatrix} t^n\cos t & x_P & 0 \\ 0 & y_P & 0 \\ 0 & z_P & t^m \end{vmatrix}}{D(t)} = \frac{y_P t^{n+m}\cos t}{D(t)} = \frac{y_P}{t^n\sin t} \\ C(t) = \dfrac{\begin{vmatrix} t^n\cos t & 0 & x_P \\ 0 & t^n & y_P \\ 0 & 0 & z_P \end{vmatrix}}{D(t)} = \frac{z_P t^{2n}\cos t}{D(t)} = \frac{z_P}{t^m\sin t} \end{cases}$$

where $t \in \mathbb{R}$, $D(t) = \begin{vmatrix} t^n\cos t & 0 & 0 \\ 0 & t^n\sin t & 0 \\ 0 & 0 & t^m \end{vmatrix} = t^{2n+m}\sin t\cos t$ and $D(t) \neq 0$ in a neighbour of t. Even if shown in the special case of a family of helices, the proce-

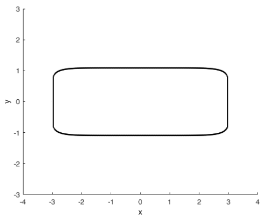

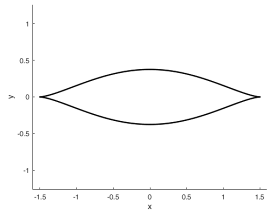

$bx^m + a^m y^m = a^m b$ $\quad$ $a^4 c^2 y^2 + (x - \frac{a}{2})^3 (x + \frac{a}{2})^3 = 0$

(a) (b)

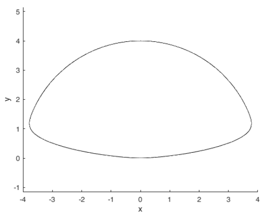

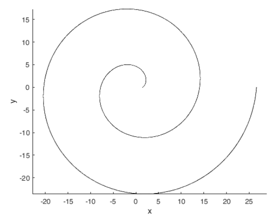

$\rho = a + b\cos^{2n}\theta$ $\quad$ $\rho = a + b\theta$

(c) (d)

Figure 3: (a) A Lamet curve with $a = 3$, $b = 2$ e $m = 8$; (b) a citrus curve with $a = 3$, $c = 1$; (c) a geometric petal (A) with $a = 4$, $b = -4$ and $n = 50$; an Archimedean spiral with $a = 1$, $b = 2$.

dure for extracting a parametric expression of $\Gamma_P(\mathcal{F})$ holds for every linear system with respect to the parameters a, b and c.

3.2 Dictionary of curves

The HT in the implicit formulation described in Section 3.1 is able to deal with a large variety of curves (e.g., besides algebraic curves also curves with a logarithmic, exponential or trigonometric representation) and, if a formulation exists, with curves expressed in parametric form. In this paper, we list a few curves used in our experiments for characteristic curves recognition; these curves complement the set proposed in [TBF18]. Finally, we highlight that additional families and combinations of curves are possible [Shi95].
In addition to the *Lamet curve*, *citrus curve*, *geometric petal (A)* and *archimedean spiral* (see Figure 3 and [TBF18] for details), the curves used in our experiments are: the *geometric petal (B)*, the *helix curve*, the *hippopede curve* and the *tennis ball curve*. The *geometric petal (B)* is a planar curve, that depends on two real parameters $a > 0$ and $b \neq 0$. Its polar equation is:

$$\rho = a + b\cos 2n\varphi$$

with $n \in \mathbb{N}$. This curve is contained in a circle with radius $a + b$ and the origin is the center of symmetry, that becomes a singular point if $a \leq |b|$ (Figure 4 (a)),

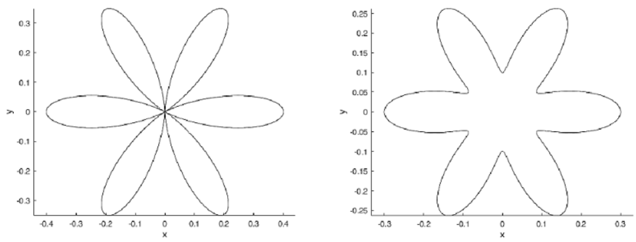

(a) (b)

Figure 4: A geometric petal (B) with (a) $a = 0.2$, $b = 0.2$, $n = 3$, (b) $a = 0.2$, $b = 0.1$, $n = 3$.

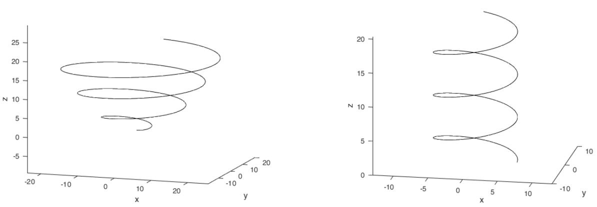

(a) (b)

Figure 5: (a) A parabolic helix with $a = 5$, $b = 4.5$ and $c = 1$; (b) a cylindrical helix with $a = 6$, $b = 5.5$ and $c = 1$.

while if $a > |b|$ there are no singularities (Figure 4 (b)). This curve is mainly used for the recognition of flowers with an even number of petals.

As already mentioned in Section 3.1 the *helix* of equation (1) is a spatial curve that depends on three real parameters a, b and c, with $c \neq 0$. Using different values of n and m, we get different families of curves. For example, if $m = n = 1$ we obtain the conical helix (Figure 2), if $m = 1$ and $n = \frac{1}{2}$ we get the parabolic helix (Figure 5 (a)), finally if $m = 1$ and $n = 0$ we obtain the cylindrical helix ((Figure 5 (b)).

The *hippopede curve* is a spatial curve that depends on two real parameters a and c. It is a special case of the sphero-cylindrical curve, represented by the intersection of a sphere centered in the origin O and radius a, and the cylinder with radius b and axis at distance c from O. If $c = a - b$ (Figure 6), we get the hippopede curve, whose implicit equation is

$$\begin{cases} x^2 + y^2 + z^2 = a^2 \\ x^2 + (z + b - a)^2 = b^2 \end{cases} .$$

Finally, our collection includes the spatial curve described by the seam line of a tennis ball with radius r. It can be seen as the intersection of two orthogonal

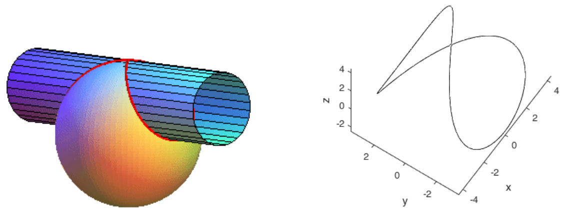

(a) (b)

Figure 6: (a) The intersection of a sphere and a cylinder; (b) a hippopede curve with $a = 4$ and $b = 3$. Figure (a) is courtesy of https://www.mathcurve.com/.

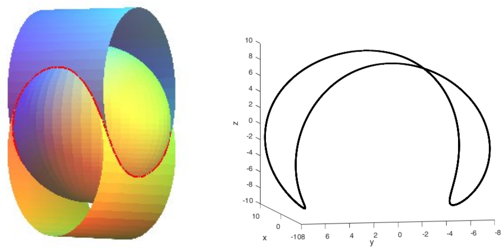

(a) (b)

Figure 7: (a) The intersection of two elliptical cylinders; (b) a tennis ball curve with $a = 8$ and $c = 2$. Figure (a) is courtesy of https://www.mathcurve.com/.

elliptical cylinders (Figure 7):

$$\begin{cases} x^2 + \frac{1}{2}(z-c)^2 = a^2 \\ y^2 + \frac{1}{2}(z-c)^2 = a^2 \end{cases}$$

where $a = \sqrt{\frac{c^2+r^2}{2}}$. This curve depends on two real parameters a and c, with $a > 0$.

4 The new method

In this paper we extend the procedure based on Hough transforms from algebraic curves described in [TBF18] both introducing a new curve aggregation method and implementing the recognition of spatial curves defined by two ipersurfaces, represented by implicit equations.

4.1 Data pre-processing

We highlight that our method does not depend on a specific characterisation method, rather it takes care of the recognition of the curves delineated by the characteristic points. We refer to [CGL*08, LZH*07] for an overview on methods for extracting characteristic points and to the SHREC benchmark for an evaluation of methods for feature curves estimation [MGM*19].

In case we are dealing with geometric curves, we adopt a mean curvature evaluation, while in case of colorimetric decorations we adopt the L-channel (luminosity) of the CIELAB space [HP11], converting the RGB values into the CIELAB ones. The mean curvature is evaluated with the curvature estimation based on normal cycles [CSM03] implemented in the Toolbox graph [Pey] in case of triangle meshes; it is approximated with the polynomial fitting of osculating jets [CP03] implemented in the CGAL package [The18] in case of point clouds. The vertices at which a property is significant (e.g with high and low property values) are selected as characteristic points. This is automatically achieved by filtering the distribution of the property values by means of two thresholds m and M. Note that m and M are two input parameters. Their value varies according to the precision threshold set for the property used to extract the feature points (e.g., in our case, two typical values of m and M are 15% and 85%, respectively).

To determine the elements that potentially correspond to a characteristic curve, the points are aggregated into clusters by adopting the *Density-Based Spatial Clustering of Applications with Noise* (DBSCAN) method [EKSX96]. The DBSCAN algorithm requires two parameters: a threshold used as the radius of the density region, and a positive integer that represents the minimum number of points required to form a dense region. To estimate the density of the feature points and, therefore, the minimum number of points in a region, the *K-Nearest Neighbor* (KNN) [FBF77] is used. In general, K is an integer number that varies from 3 to 15.

4.2 Curves approximation using Hough transforms

Once we have aggregated the points, we apply to each single group the HT recognition technique. If the potential characteristic curve can be locally flattened onto a plane without any overlap, it is projected onto the best fitting plane. Such a plane is defined as the multiple linear regression plane of the set of points and computed with the least square method. In this case, for recognition purposes, it is enough to consider a family of planar curves, otherwise we select a family of spatial curves.

The peculiarity of the HT is to estimate in a family of curves, the parameters of the curve $\mathbf{a} = (a_1, \dots, a_n)$ that better approximates a given set of points. The curves considered in this paper have one, two or three parameters. Depending on the curve, these parameters estimate its bounding box, diagonal, radius, etc. Figure 8 represents the curve fitting in the space of parameters obtained for a hyppopede and a helix curve. The procedure to find the parameters consists of three steps:

1. Fix a bounded region $\mathcal{T}$ of the parameter space by exploiting typical characteristics of the chosen family of curves and fix a discretization of $\mathcal{F}$ (for details see [TBF18]).

2. Build an accumulator matrix, whose entries represent the cells. The Hough

transforms of points of interest are then evaluated and the matrix is updated by placing each entry of the matrix equal to the number of transforms passing through the cell corresponding to this entry. For the evaluation, we adopt the method theoretically proved in [TBS18], which is based on the bounds evaluation of a given locus $V(F)$, with $F = (f_1, ..., f_m)$, w.r.t a cell centered at P with radius ε (f_j, $j = 1, ..., m$, are analytic functions on an open convex set $U \in \mathbb{R}^n$). Such bounds depend on the Jacobian of F Jac_F and the Hessian matrices of f_j H_{f_j}, $j = 1, ..., m$. They are defined as follows:

$$B_1 = \|Jac_F(P)\|_\infty \varepsilon + \frac{n}{2}\varepsilon^2 H^\infty,$$

$$B_2 = \frac{2R}{J^\infty(2 + mnRJ^\infty H^\infty)}$$

where $H^\infty := \|(H_1, ..., H_m)^t\|_\infty$,
with $H_j := max_{\{x \in \mathbb{R}^n \mid \|(x-P)^t\|_\infty \leq \varepsilon\}} \left\|H_{f_j}(x)\right\|_1$,
$J^\infty := max_{\{x \in \mathbb{R}^n \mid \|(x-P)^t\|_\infty \leq \varepsilon\}} \left\|Jac_F^\dagger(x)\right\|_\infty$,
with $Jac_F^\dagger$ denoting the Moore-Penrose pseudo-inverse of Jac_F, and $R < min\{\varepsilon, \frac{\sigma}{\sqrt{mnH^\infty}}\}$, with σ the smallest singular value of $Jac_F(P)$. Since the above quantities depend on the Jacobian and the Hessian matrices, P must be a point for which these values are non-trivial. In our method we use the system *CoCoA* [ABL] for the symbolic manipulation of matrices.

3. Identify the entry that corresponds to the maximum value of the accumulator matrix and return the coordinates of its center, which correspond to the parameters of the curve of the family that best approximates the feature curve. If there is more than one entry assuming the maximum value, more curves are potential solutions of the HT and are evaluated.

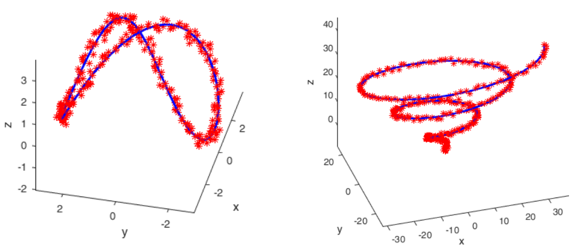

(a) (b)

Figure 8: Curve fitting through Hough transform of a hippopede (a) and a helix (b) curve. In these examples the points come from a parametric expression of the curves locally perturbed with a 5% Gaussian noise.

4.3 Compound curves

Our method also allows the recognition of compound curves (Figure 9), in two different ways: the first builds a new family of curves defined by the product of the equations of the curves of the families composing it; the second aggregates these curves exploiting previous knowledge.

Figure 9(a) represents the HT fitting of a part of a Greek fret with 8 straight lines. In this case, the lines are orthogonal to the Cartesian axes and therefore, the degree of the HT curve is still limited. In general, the product approach can deal with curves of very high degree (for instance, a flower with 6 petals recognised with a citrus curve of degree 3, would generate a HT transform of degree 18).

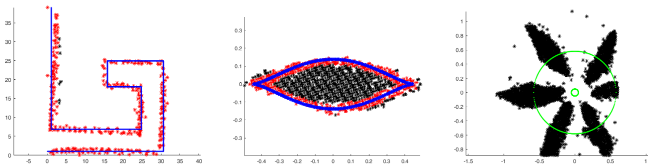

(a) (b) (c)

Figure 9: Two examples of compound curves. (a) The curve is recognised as the product of 8 straight lines. (b) The six-petal flower is seen as the union of six citrus-like curves and it is located because one of the extremities of these petal have to lie between the circles in green.

For this reason, we aim at automatic modelling the rules and parameters that characterise a style element and replicate them with the same rule. In particular, we are able to recognise the decorations made of elements that are repeated in the space in a geometric way, locating the individual components and then aggregating them according to decoration-specific rules. For instance, in the case of the six-petal flower that characterises many fragments of votive statues from the Salamis island [STA], we have identified the following recognition steps:

1. the extraction of the feature points, i.e., the vertices of the model with a high luminosity value, given the peculiarity of a light decoration over a dark background [KKF91];

2. the recognition of each single petal with the citrus curve family, thus obtaining the parameters in the coordinates of the salient points of this curve, i.e. the endpoints of the curve symmetry axes ((Figure 9(b));

3. the evaluation of the rays of the circular crown within which the salient points have to lie if the petals belong to the same flower (Figure 9 (c)).

4.4 Curve distance estimation

The distance between the two curves $\mathcal{C}_1$ and $\mathcal{C}_2$ is defined as the norm L^1 of the parameters corresponding to these curves, i.e., $d(\mathcal{C}_1,\mathcal{C}_2) = |\mathbf{a}_{\mathcal{C}_1},\mathbf{a}_{\mathcal{C}_2}|_1$, where $\mathbf{a}_{\mathcal{C}_1}$

and $\mathbf{a}_{\mathcal{C}_2}$ are the parameters of the curves $\mathcal{C}_1$ and $\mathcal{C}_2$, respectively.

Note that such a notion of distance assumes that the curve parameters are homogeneous in terms of the properties measured; this implies that the distance between two characteristic curves is computed only if they belong to the same family.

4.5 Evaluation

To determine if a curve satisfactorily approximates the set of characteristic points, we use the notion of *Goodness of Fit* (GoF), [MPCB15]. Let m be the maximum value reached by the accumulation matrix and let *perc* be a percentage of m chosen in relation to the conditions of the problem to be solved. Let $\mathcal{T}'$ a region subset of $\mathcal{T}$ consisting of the cells corresponding to the entries of the accumulation matrix whose value is greater than this percentage. At this point, we define a subset of the initial cluster's points that contains the "good" points, that is the points P_s such that $\Gamma_{P_s}(\mathcal{F}) \cap \mathcal{T}' \neq \emptyset$. Let S be the set of these points. Let d_s be the Euclidean distance of the point P_s from the curve $\mathcal{C}$, given by $d_s = d(P_s, \mathcal{C}) = inf_{P \in \mathcal{C}} \| P_s - P \|_2$. Then the measure of recognition reliability is defined as follows:

$$GoF := \frac{d_1 + d_2 + ... + d_{\sharp S}}{\sharp S},$$

where $\sharp S$ is the cardinality of the set S. The curve $\mathcal{C}$ is a good recognition if the value of GoF is small compared to a given threshold that depends on the context (for example if it is small compared to the order of magnitude of the parameters).

Computational cost Similarly to the HT of curves expressed in a parametric form, the cost of the HT detection algorithm described in Section 4 is dominated by the size of the discretization of the region of the parameters. Such a discretization consists of $M = \prod_{k=1}^{t} J_k$ elements, where t is the number of parameters (in the curves proposed in this paper, $t = 1, 2, 3$) and J_k is the number of subdivisions for the kth parameter. In case the curves are in implicit form, we need to evaluate, once for each curve, the symbolic expression of the Jacobian, the Moore-Penrose pseudo-inverse and Hessian matrices; therefore, even if the the cost of fitting a curve has the same computational complexity in both cases, for parametric curves the HT implementation is more intuitive.

5 Experimental results

Our method has been tested on models collected from the web: the Turbosquid repository [Tur], the AIM@SHAPE repository [VIS15], the STARC repository [STA] and the benchmark proposed in the *SHape REtrieval Contest SHREC'19* (SHREC'19) track on feature curve extraction [MGM*19].

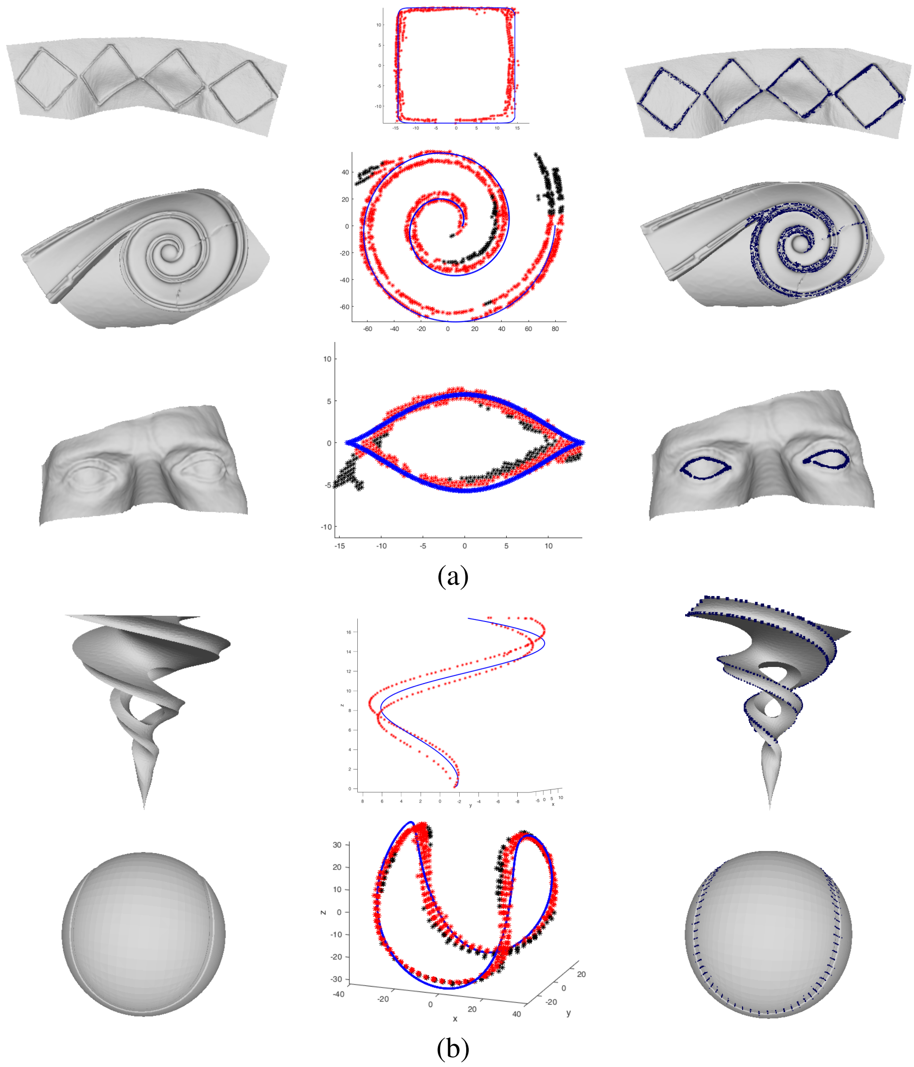

Figure 10: (a) Characteristic curves recognised using a family of planar curves, respectively a Lamet curve, an Archimedean spiral and a citrus curve; (b) characteristic curves recognised with a family of spatial curves, respectively helix curves and a tennis ball curve

5.1 Recognition of characteristic curves

Figure 10 (a) shows the results obtained on some of the models of artefacts proposed as benchmark for the SHREC'19 contest on feature-curve recognition [MGM*19]. Once the feature points are grouped in a set of potential curves, to each group we apply the curve recognition method described in Section 4. For most of these models it was possible to locally project the groups onto a plane and then, to recognise them with a family of planar curves. The central and right columns of Figure 10 show, respectively, the recognition of one of the characteristic curves extracted from the corresponding model and the feature points recognised on the model. In the case of the shell-like model in Figure 1, we recognise the main style element with a helix, i.e., a spatial curve. Figure 10 (b) presents further examples of recognition of spatial curves on man-made objects. On the first model it was possible to recognise two style elements, using the family of helices given by the equation

$$\begin{cases} x = at^{\frac{1}{5}} \cos t \\ y = bt^{\frac{1}{5}} \sin t \qquad t \in \mathbb{R}. \\ z = ct^{\frac{3}{5}} \end{cases}$$

On the second model the curve outlined by the seam of the tennis ball was recognised with the family of curves

$$\begin{cases} x^2 + \frac{1}{2}(z-c)^2 = a^2 \\ y^2 + \frac{1}{2}(z-c)^2 = a^2 \end{cases}$$

of our dictionary.

5.2 Aggregation of characteristic curves

We recognised compound curves via repeated, aggregation rules, on several architectural decorations and archaeological fragments. Here we show two examples of decorative elements: a frieze of flowers repeated in space (floral band) and a Greek fret. The recognition of the flowers of a floral band has been performed on the basis of the rules described in Section 4.3. In this way, it is possible to recognise decorative flowers with a number of petals greater than or equal to 4 (Figure 11). On the basis of their contiguity, we can aggregate them so that we can recognise the whole floral band.

To recognise the Greek fret, we firstly identified a single style elements as the product of 8 straight lines, thus constructing a suitable family of curves defined as product of equations of lines (Figure 9 (a)). Since these style elements are represented as geometric reliefs, the characteristic points are detected through the mean curvature values. Finally, with the parameters obtained for the single style element, it has been possible to recognise the entire Greek fret (Figure 12 (b)) by translating the single element.

5.3 Compatibility of characteristic curves

The curve parameters obtained through the HT technique are natural indicators of the most representative curve and therefore they can be used to compare curves belonging to the same family, even if they have been recognised on different objects. These parameters suggest insights on the style compatibility of the objects themselves. Figure 13 shows examples of parts to which we have applied our method

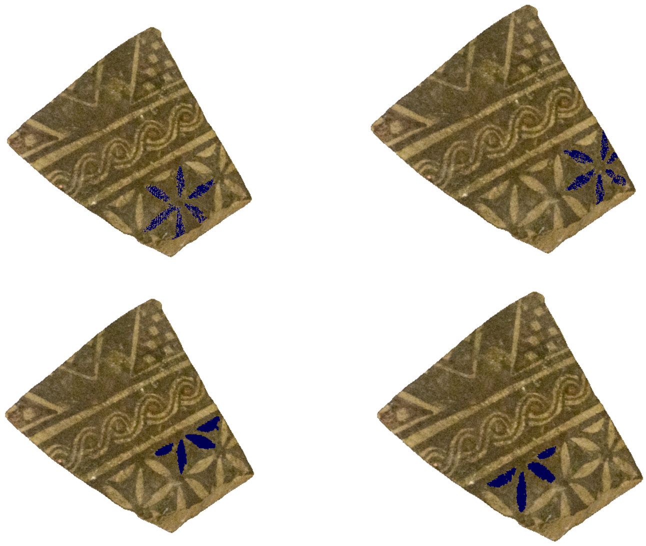

(1)

(2)

Figure 11: Two examples of floral band. In (1) we recognised 4 flowers, with six and four petals, respectively; in (2) we recognised 3 flowers, with six or five petals.

and, thanks to the elements recognised, we have been able to compare in term of style elements. For recognising the sets of characteristic points in Figure 13(a) we have used the family of Archimedean spirals; the parameters (a,b) found by our method have been compared as explained in Section 4.4. In Figure 13(a), the parts are sorted in increasing order of distance from the leftmost one (that acts as the query set). These parts come from different models proposed in SHREC'19 benchmark [MGM*19]. In particular, looking at the two closest spirals, we noticed that the two characteristic curves could be part of the same ornament (Figure 13 (b)). Similarly, for the fragments in Figure 13 (c) we successfully recognised the eyes with curves of the citrus family and we noticed that these eyes could belong to the same statue.

Finally, Figure 14 shows four different fragments, potentially coming from different votive statues but all with the same stylistic character of a floral band. We decided to compare these fragments by recognising the 6-petal flowers in the floral

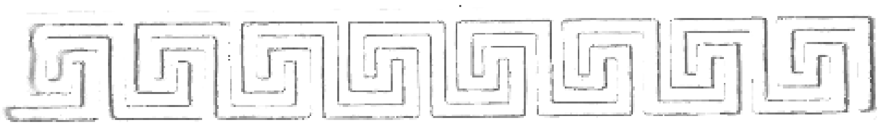

(a)

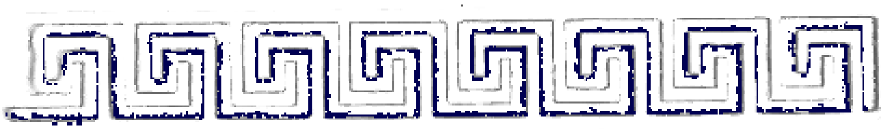

(b)

Figure 12: (a) A digital model of a Greek fret; (b) the recognition of the entire Greek fret.

band (i.e., the output of the aggregation procedure detailed in Section 5.2) with the family of curves geometric petal (B). As can be seen in Figure 14 (b), the recognition is not always perfect since the flowers have been drawn by hand and therefore inaccurate, while the family of curves follows precise geometric rules. Despite this, the parameters we obtain give enough information on the size of the flowers and through these it is possible to construct a similarity matrix that allows us to compare the recognised flowers (Figure 14 (c)). Finally, to compare the models we can average the distances of the flowers that make up their floral bands or take the minimum of them (Figure 14 (d)). In this way it was possible to conclude that the floral bands present on the fragments (1), (3) and (4) are similar and therefore they could belong to the same statue, while the one in the fragment (2) is different.

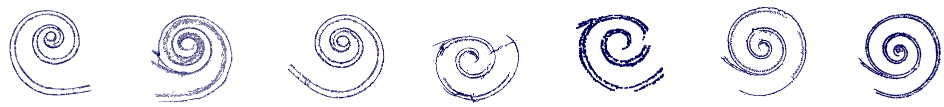

query d=0.0638 d=0.1529 d=0.3391 d=0.4705 d=0.7976 d=1

(a)

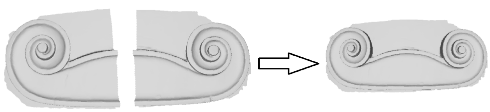

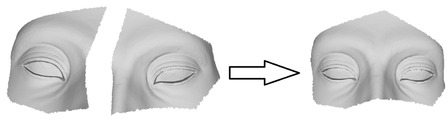

(b) (c)

Figure 13: (a) A curve in input and the most similar curves found with respect to their increasing distance. The most similar curves interpreted as parts of the same ornament in (b) or the same mask in (c).

(1) (2) (3) (4)

(a)

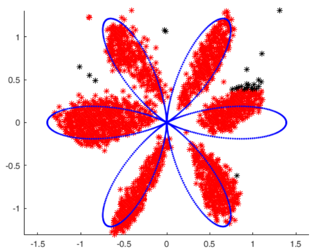

(b)

	1_1	2_1	3_1	1_2	2_2	1_3	1_4	2_4
1_1	0	0.2040	0.0760	0.5535	0.4615	0.0524	0.2657	0.0867
2_1	0.2040	0	0.1280	0.7575	0.6655	0.2564	0.0617	0.2147
3_1	0.0760	0.1280	0	0.6295	0.5375	0.1284	0.1897	0.0867
1_2	0.5535	0.7575	0.6295	0	0.0920	0.5039	0.7218	0.5428
2_2	0.4615	0.6655	0.5375	0.0920	0	0.4119	0.6298	0.4508
1_3	0.0524	0.2564	0.1284	0.5039	0.4119	0	0.3181	0.1391
1_4	0.2657	0.0617	0.1897	0.7218	0.6298	0.3181	0	0.1790
2_4	0.0867	0.2147	0.0867	0.5428	0.4508	0.1391	0.1790	0

(c)

	distanza media	distanza minima
Modelli 1 e 2	0.6008	0.4615
Modelli 1 e 3	0.1457	0.0524
Modelli 1 e 4	0.1509	0.0617
Modelli 2 e 3	0.4579	0.4119
Modelli 2 e 4	0.5863	0.4508
Modelli 3 e 4	0.2286	0.1391

(d)

Figure 14: (a) Four different fragments with the same stylistic character of a floral band; (b) flower with 6 petals recognised with a geometric petal (B) curve; (c) similarity matrix of the flowers recognised on the four models; (d) medium and minimum distance between the models.

5.4 Concluding remarks

This paper describes a new method to recognise characteristic curves on 3D shapes. As shown in the examples, this technique has been successfully applied to the recognition of style elements represented by simple curves or their composition, even in the presence of noise or incompleteness. We approximate these curves with known curves using a generalisation of the HT able to deal with curves represented either in implicit and parametric form. As demonstrated, the method allows new additions of curves in the catalogue of functions already available and supports the definition of new rules of composition or aggregation of characteristic curves to recognise compound patterns.

To the best of our knowledge, it is the first method for the recognition via HT of spatial curves. Indeed, previous HTs for 3D were limited to surface recognition, such as planes, spheres or ellipsoids. Our method suggests a generic strategy to deal with characteristic curves represented in terms of the intersection of two or more surfaces. Till now, the approximation of profiles or style elements with spatial curves was limited to spline fitting or to specific families of curves with ad-hoc methods, such as the 3D Euler spiral [HT11]. In the case of Hough transforms, the same framework easily generalises to more generic families of curves. If the style elements can be projected onto a plane, their characteristic curves can be handled as planar curves: in this way we can take advantage of large dictionaries of curves, while for spatial curves such facilities do not yet exist.

The most appealing property of the HT is its ability of recognising a curve profile (and therefore a style element) in its entirety, even in presence of noise and partial data: this implies that the HT is naturally suitable for shape completion and multiple curve and pattern comparison. Its strength is also its main limitation: to be effective, the families of curves used for the HT must include a curve that somehow resembles the style element to be recognised.

Recently, the HT has been proposed also for the fitting of low-degree piece-wise polynomial curves [CRS18] in images. In this case, the outcome is a spline curve approximating a profile image that consists of polynomial pieces connected G^1 continuously, except in correspondence of cusps, where the order of continuity is only C^0. Although piece-wise splines of low degree polynomials are the most common curves that can be combined to construct a spatial curve, low degree polynomials cannot span a large number of points, therefore many small segments need to be blended together to build the desired curve and such a decomposition is not unique.

References

[ABL] ABBOTT J., BIGATTI A. M., LAGORIO G.: CoCoA-5: a system for doing Computations in Commutative Algebra. Available at http://cocoa.dima.unige.it.

[APM15] ANDREADIS A., PAPAIOANNOU G., MAVRIDIS P.: Generalized digital reassembly using geometric registration. In *Digital Heritage* (2015), vol. 2, pp. 549–556.

[Bal81] BALLARD D. H.: Generalizing the Hough transform to detect arbitrary shapes. *Pattern recognition 13*, 2 (1981), 111–122.

[BLL15] BUGLIO D. L., LARDINOIS V., LUCA L. D.: What do thirty-one columns say about a “theoretical” thirty-second? *J. Comput. Cult. Herit. 8*, 1 (Feb. 2015), 6:1–6:18.

[BMP13] BELTRAMETTI M., MASSONE A., PIANA M.: Hough transform of special classes of curves. *SIAM J. Imaging Sci. 6*, 1 (2013), 391–412.

[BR12] BELTRAMETTI M. C., ROBBIANO L.: An algebraic approach to Hough transforms. *J. of Algebra 37* (2012), 669–681.

[CGL*08] COLE F., GOLOVINSKIY A., LIMPAECHER A., BARROS H. S., FINKELSTEIN A., FUNKHOUSER T., RUSINKIEWICZ S.: Where do people draw lines? *ACM Trans. Graph. 27*, 3 (Aug. 2008), 1–11.

[CP03] CAZALS F., POUGET M.: Estimating differential quantities using polynomial fitting of osculating jets. In *Proc. of the 2003 EG/ACM SIGGRAPH Symp. on Geometry Processing* (2003), pp. 177–187.

[CRS18] CONTI C., ROMANI L., SCHENONE D.: Semi-automatic spline fitting of planar curvilinear profiles in digital images using the hough transform. *Pattern Recogn. 74*, C (Feb. 2018), 64–76.

[CSM03] COHEN-STEINER D., MORVAN J.-M.: Restricted Delaunay triangulations and normal cycle. In *Proc. of the* 9^{th} *Ann. Symp. on Computational Geometry* (New York, NY, USA, 2003), SCG '03, ACM, pp. 312–321.

[DH72] DUDA R. O., HART P. E.: Use of the Hough transformation to detect lines and curves in pictures. *Commun. ACM 15*, 1 (1972), 11–15.

[DIOHS08] DANIELS II J., OCHOTTA T., HA K. L., SILVA T. C.: Spline-based feature curves from point-sampled geometry. *The Visual Computer 24*, 6 (2008), 449–462.

[DKVL16] DEV K., KIM K., VILLAR N., LAU M.: Improving style similarity metrics of 3d shapes. In *Proceedings of the 42Nd Graphics Interface Conference* (School of Computer Science, University of Waterloo, Waterloo, Ontario, Canada, 2016), GI '16, Canadian Human-Computer Communications Society, pp. 175–182.

[DSG*12] DOERSCH C., SINGH S., GUPTA A., SIVIC J., EFROS A. A.: What makes Paris look like Paris? *ACM Trans. Graph. 31*, 4 (July 2012), 101:1–101:9.

[EKSX96] ESTER M., KRIEGEL H. P., SANDER J., XU X.: A density-based algorithm for discovering clusters in large spatial databases with noise. In 2^{nd} *Int. Conf. Knowledge Discovery and Data Mining* (1996), AAAI Press, pp. 226–231.

[Far93] FARIN G.: *Curves and Surfaces for Computer Aided Geometric Design (3rd Ed.): A Practical Guide*. Academic Press Professional, Inc., San Diego, CA, USA, 1993.

[FBF77] FRIEDMAN J. H., BENTLEY J. L., FINKEL R. A.: An algorithm for finding best matches in logarithmic expected time. *ACM Trans. Math. Softw. 3*, 3 (Sept. 1977), 209–226.

[HLK*17] HU R., LI W., KAICK O. V., HUANG H., AVERKIOU M., COHEN-OR D., ZHANG H.: Co-locating style-defining elements on 3d shapes. *ACM Trans. Graph. 36*, 3-4 (June 2017).

[Hou62] HOUGH P. V. C.: Method and means for recognizing complex patterns, 1962. US Patent 3,069,654.

[HP11] HUNT R. W. G., POINTER M. R.: *Measuring Colour, Fourth Edition*. Wiley, 2011.

[HT11] HARARY G., TAL A.: The Natural 3D Spiral. *Computer Graphics Forum 30*, 2 (2011), 237–246.

[HT12] HARARY G., TAL A.: 3D Euler spirals for 3D curve completion. *Computational Geometry 45*, 3 (2012), 115 – 126.

[KKF91] KARAGEORGHIS V., KARAGEORGHIS J., FOUNDATION A. L.: *The coroplastic art of ancient Cyprus*. Nicosia : A.G. Leventis Foundation, 1991. At head of title: A.G. Leventis Foundation.

[KST08] KOLOMENKIN M., SHIMSHONI I., TAL A.: Demarcating curves for shape illustration. *ACM Trans. Graph. 27*, 5 (2008), 157:1–157:9.

[KTT99] KASSIM A., TAN T., TAN K.: A comparative study of efficient generalised Hough transform techniques. *Image and Vision Computing 17*, 10 (1999), 737 – 748.

[KZHCO11] KAICK O. V., ZHANG H., HAMARNEH G., COHEN-OR D.: A Survey on Shape Correspondence. *Computer Graphics Forum* (2011).

[Lip69] LIPSCHUTZ M.: *Schaum's Outline of Differential Geometry*. Schaum's Series. McGraw-Hill Education, 1969.

[LKS15] LUN Z., KALOGERAKIS E., SHEFFER A.: Elements of style: Learning perceptual shape style similarity. *ACM Trans. Graph. 34*, 4 (July 2015), 84:1–84:14.

[LKWS16] LUN Z., KALOGERAKIS E., WANG R., SHEFFER A.: Functionality preserving shape style transfer. *ACM Trans. Graph. 35*, 6 (Nov. 2016), 209:1–209:14.

[LWWS15] LI C., WAND M., WU X., SEIDEL H. P.: Approximate 3d partial symmetry detection using co-occurrence analysis. In *2015 International Conference on 3D Vision* (Oct 2015), pp. 425–433.

[LZH*07] LAI Y. K., ZHOU Q. Y., HU S. M., WALLNER J., POTTMANN H.: Robust feature classification and editing. *IEEE Transactions on Visualization and Computer Graphics 13*, 1 (Jan 2007), 34–45.

[LZH*17] LUN Z., ZOU C., HUANG H., KALOGERAKIS E., TAN P., CANI M.-P., ZHANG H.: Learning to group discrete graphical patterns. *ACM Trans. Graph. 36*, 6 (Nov. 2017), 225:1–225:11.

[MC15] MUKHOPADHYAY P., CHAUDHURI B. B.: A survey of Hough transform. *Pattern Recognition 48*, 3 (2015), 993 – 1010.

[MGM*19] MOSCOSO THOMPSON E., GERASIMOS A., MOUSTAKAS K., NGUYEN E. R., TRAN M., LEJEMBLE T., BARTHE L., MELLADO N., ROMANENGO C., BIASOTTI S., FALCIDIENO B.: SHREC'19 track: Feature Curve Extraction on Triangle Meshes. In *Eurographics Workshop on 3D Object Retrieval* (2019), Biasotti S., LavouÃl' G., Falcidieno B., Pratikakis I., (Eds.), The Eurographics Association.

[MPCB15] MASSONE A., PERASSO A., CAMPI C., BELTRAMETTI M.: Profile detection in medical and astronomical images by means of the hough transform of special classes of curves. *J. Math. Imaging Vis.* (2015), 296–310.

[MPWC12] MITRA N. J., PAULY M., WAND M., CEYLAN D.: Symmetry in 3d geometry: Extraction and applications. In *EUROGRAPHICS State-of-the-art Report* (2012).

[MTB18] MOSCOSO THOMPSON E., BIASOTTI S.: Description and retrieval of geometric patterns on surface meshes using an edge-based lbp approach. *Pattern Recognition 82* (2018), 1 – 15.

[MTB19] MOSCOSO THOMPSON E., BIASOTTI S.: Retrieving color patterns on surface meshes using edgelbp descriptors. *Computers & Graphics 79* (2019), 46 – 57.

[OLA14] OESAU S., LAFARGE F., ALLIEZ P.: Indoor Scene Reconstruction using Feature Sensitive Primitive Extraction and Graph-cut. *ISPRS J. of Photogrammetry and Remote Sensing 90* (Mar. 2014), 68–82.

[Pey] PEYRE G.: Toolbox graph - A toolbox to process graph and triangulated meshes. http://www.ceremade.dauphine.fr/∼peyre/matlab/graph/content.html.

[PT97] PIEGL L., TILLER W.: *The NURBS Book (2Nd Ed.)*. Springer-Verlag New York, Inc., New York, NY, USA, 1997.

[Ran81] RANDALL H.: A consideration of style in archaeology. *Arizona Anthropologist 2* (1981), 13–39.

[RES16] RODRIGUEZ ECHAVARRIA K., SONG R.: Analyzing the decorative style of 3d heritage collections based on shape saliency. *J. Comput. Cult. Herit. 9*, 4 (Dec. 2016), 20:1–20:17.

[Shi95] SHIKIN E. V.: *Handbook and atlas of curves*. CRC, 1995.

[SJW*11] SUNKEL M., JANSEN S., WAND M., EISEMANN E., SEIDEL H.-P.: Learning line features in 3D geometry. *Computer Graphics Forum (Proc. EUROGRAPHICS) 30*, 2 (April 2011).

[STA] STARC repository. http://public.cyi.ac.cy/starcRepo/.

[Tal14] TAL A.: *3D Shape Analysis for Archaeology*. Springer Berlin Heidelberg, Berlin, Heidelberg, 2014, pp. 50–63.

[TB14] TORRENTE M.-L., BELTRAMETTI M. C.: Almost vanishing polynomials and an application to the Hough transform. *J. of Algebra and Its Applications 13*, 08 (2014), 1450057.

[TBF18] TORRENTE M.-L., BIASOTTI S., FALCIDIENO B.: Recognition of feature curves on 3D shapes using an algebraic approach to hough transforms. *Pattern Recognition 73* (2018), 111 – 130.

[TBS18] TORRENTE M., BELTRAMETTI M., SENDRA J.: r-norm bounds and metric properties for zero loci of real analytic functions. *J. of Computational and Applied Mathematics 336* (2018), 375 – 393.

[The18] THE CGAL PROJECT: *CGAL User and Reference Manual*, 4.13 ed. CGAL Editorial Board, 2018. URL: https://doc.cgal.org/4.13/Manual/packages.html.

[Tur] Turbosquid. https://www.turbosquid.com/3d-model.

[VIS15] The Shape Repository. http://visionair.ge.imati.cnr.it/ontologies/shapes/, 2011–2015.

Recent titles from the IMATI-REPORT Series:

2018

18-01: *Arbitrary-order time-accurate semi-Lagrangian spectral approximations of the Vlasov-Poisson system*, L. Fatone, D. Funaro, G. Manzini.

18-02: *A study on 3D shape interaction in virtual reality*, E. Cordeiro, F. Giannini, M. Monti, A. Ferreira.

18-03: *Standard per la gestione e procedure di validazione di dati meteo da sensori eterogenei e distribuiti,* A. Clematis, B. Bonino, A. Galizia.

18-04: *Strumenti e procedure per la gestione e la visualizzazione di dati meteo prodotti da sensori eterogenei e distribuiti tramite interfacce web basate su mappe geografiche,* L. Roverelli, G. Zereik, B. Bonino, A. Gallizia, A. Clematis.

18-05: *TopChart: from functions to quadrangulations*, T. Sorgente, S. Biasotti, M. Livesu, M. Spagnuolo.

18-06: *Adaptive sampling of enviromental variables (ASEV*), S. Berretta, D. Cabiddu, S. Pittaluga, M. Mortara, M. Spagnuolo, M. Vetuschi Zuccolini.

18-07: *Multi-criteria similarity assessment for CAD assembly models retrieval*, K. Lupinetti, F. Giannini, M. Monti, J,-P. Pernot.

18-08: *IGA-based Multi-Index Stochastic Collocation for random PDEs on arbitrary domains*, J. Beck, L. Tamellini, R. Tempone

18-09: *High order VEM on curved domains*, S. Bertoluzza, M. Pennacchio, D. Prada.

18-10: *Estimation of the mortality rate functions from time series field data in a stage-structured demographic model for Lobesia botrana,* S. Pasquali, C. Soresina.

2019

19-01: *Feature curves, Hough transform, characteristic elements*, C. Romanengo, S. Biasotti, B. Falcidieno.